A 3D Framework for Quantifying and Geovisualizing Window-View Green Visibility from Simulated Indoor Perspectives

Zongrong Li[1]*, Lei Zou[1]* and Jinsil Hwaryoung Seo [2]

[1] Department of Geography, Texas A&M University, College Station, TX
[2] Department of Visualization, Texas A&M University, College Station, TX
* lzou@tamu.edu

Keywords: window-view greenery, WGVI, built environment, urban vegetation, 3D urban analysis

Introduction

Visible urban greenery reduces stress and supports cognition and emotional restoration, and regular visual contact with vegetation is associated with lower depression and anxiety (Elsadek et al., 2020; Yan et al., 2023). Yet most greenness assessments rely on overhead indices rather than the human viewpoint, and street-view imagery, while eye-level (Biljecki & Ito, 2021), still omits indoor perspectives such as window views.

As individuals spend roughly 70%–90% of their time indoors (Klepeis et al., 2001), window views are an important connection to nature. Prior work has measured window-level greenery through manual photography (Lin et al., 2022), LiDAR-based visibility simulation (Bolte et al., 2024), and mesh-based photorealistic rendering (Li et al., 2022), but at single-building or district scale. LiDAR captures geometry without appearance, so it cannot separate canopy from other surfaces in the visible scene, and its coverage is uneven; photorealistic 3D tiles offer consistent coverage supporting city-scale, transferable analysis.

To address this gap, this study proposes an integrated 3D framework to quantify the Window-Level Green View Index (WGVI) from simulated indoor perspectives. Focusing on Houston, Texas, the analysis covers 48,398 buildings sampled from 622,600 city-wide, yielding 921,162 window-view renderings. Two hypotheses are tested: (H1) WGVI varies systematically with floor height due to visual obstruction and built environment context; and (H2) built environment and vegetation jointly shape WGVI across building types and floor levels.

Method

The framework comprises four steps: single-building localization, viewpoint calculation, semantic segmentation, and statistical analysis relating WGVI to environmental variables.

Single-Building Localization

A Single-Building Localization algorithm aligns GlobalBuildingAtlas footprints with Google Photorealistic 3D Tiles (Figure 1).

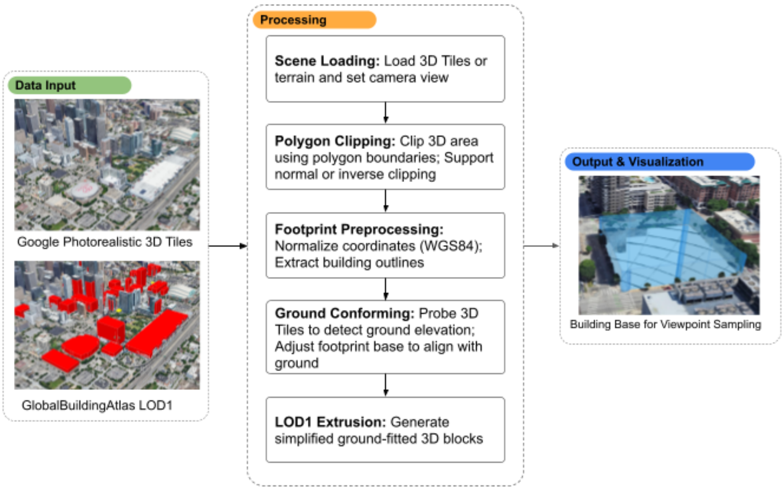

Figure 1: Single-Building Localization Algorithm

The 3D scene is loaded, the area is clipped, and footprint vertices are adjusted using 3D Tiles elevation. For each vertex i, the adjustment is computed as Equation (1):

$$\hat{v}_i = P_i + n_i d_p - n_i d_b \tag{1}$$

where $P_i$is the original vertex, $n_i$the outward unit normal, $d_p$the probing distance, and d_b the backoff offset. After alignment, watertight LOD1 blocks are generated for viewpoint sampling.

Viewpoint Calculation

Building on the localized models, we generate observation points and simulate façade perspectives (Figure 2).

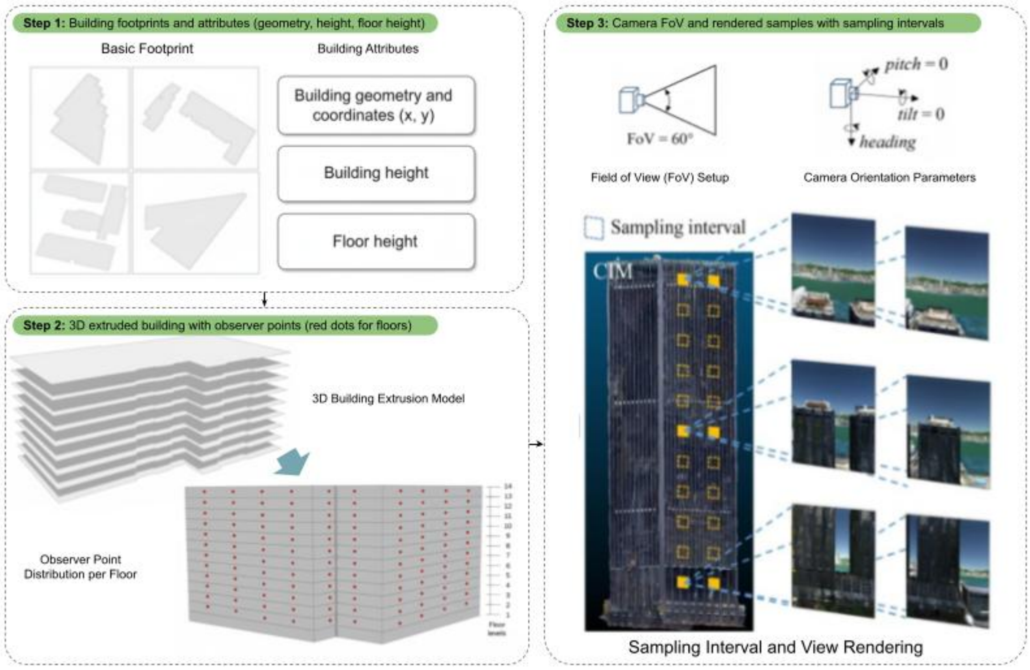

Figure 2: Viewpoint calculation for façade rendering, showing observer spacing along the façade and the outward camera orientation.

We extract building geometry and height from GlobalBuildingAtlas and extrude LOD1 models. Observer points are spaced along each façade by façade length (5 m below 20 m, 10 m for 20–50 m, 20 m above 50 m), inset 3 m from corners, and offset 0.8 m outward along the façade normal. Vertical positions are computed as

$$z_k = k \times h_f + h_0 + h_e \tag{2}$$

where h_f is floor height, h_0 ground elevation, and h_e the eye height (1.5 m).

Floor height is 3.0 m and the camera sits 1.5 m above each slab, so the viewpoint labelled floor k lies at h_0 + 3.0k + 1.5 m and represents storey k+1; the topmost sample of each building therefore sits about 1.4 m above its roof. Cameras face outward along the façade normal, pitch and roll at 0°, with a 60° field of view following Li et al. (2022). Not every storey is rendered: low-rise buildings contribute floors 1 and 2, mid-rise floors 1 and 3–10, and high-rise floors 1, 4, 7, 10 and above.

Semantic Segmentation

We apply semantic segmentation to façade images, classifying pixels into vegetation, water, sky, and building (Figure 3). A DeepLabv3+ model pre-trained on Cityscapes and fine-tuned on the CIM-WV window-view dataset (Li et al., 2024) achieves a mean IoU of 0.879 on that benchmark. As CIM-WV derives from Hong Kong, transfer to Houston remains a source of uncertainty.

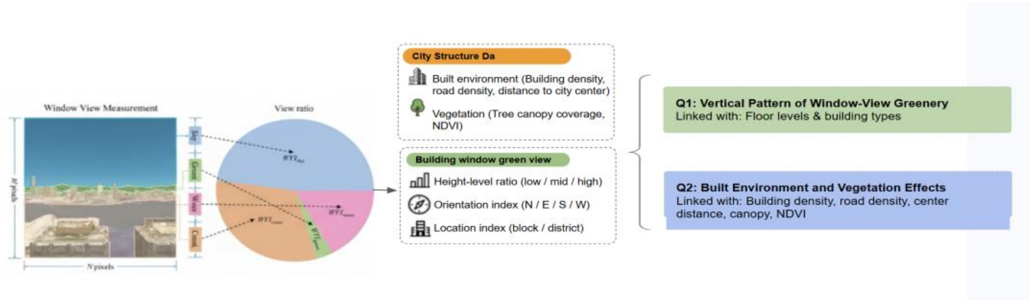

Figure 3: Semantic Segmentation and Analysis Framework.

For each façade image $I_i$of size $H \times W$, the model produces a pixel-wise semantic label map S_i. The view ratio for each class $c$is calculated as

$$WV_i^{(c)} = \frac{N_c}{N_{total}} \tag{3}$$

where $N_c$is the number of pixels in class $c$and $N_{total}$the total number of valid pixels. These ratios form the Window-Level Green View Index (WGVI), aggregated by building and floor level.

Results

Study Area and Data

This study focuses on Houston, Texas (~4,600 km²; Figure 4). Building data come from GlobalBuildingAtlas (Zhu et al., 2025). Following He et al. (2019), the 622,600 buildings are classified as low-rise (<9 m; 1–2 floors), mid-rise (9–30 m; 3–10 floors), and high-rise (>30 m; >10 floors). We stratify-sample about 10% of low- and mid-rise buildings by ZIP code and retain all high-rise buildings. After failed renders are dropped, the analysed set is 48,398 buildings (33,461 low-, 12,850 mid-, 2,087 high-rise), 98,368 building-floor records and 921,162 viewpoints. Tiles come from the Google Map Tiles API and are used only as textured geometry, so the pipeline can be re-run on LiDAR-derived meshes or open 3D city models.

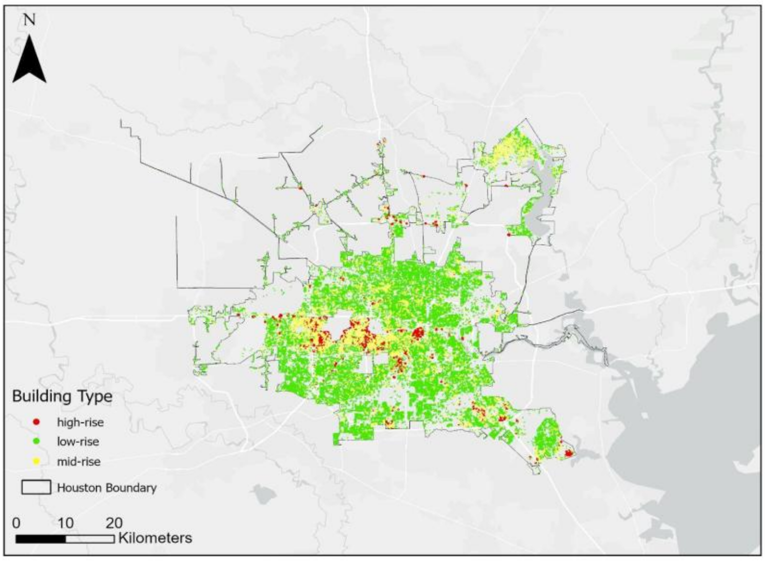

Figure 4: Distribution of buildings across Houston, Texas.

To examine how urban form and vegetation influence WGVI, we integrate built environment variables following the 5Ds framework and vegetation indicators including tree canopy coverage and distance to green space (Table 1).

Category	**Variable**	**Data Source**
Built environment (5Ds)	Building height	Global Human Settlement Layer (GHSL)
Built environment (5Ds)	Land-use diversity	Land-use dataset
Built environment (5Ds)	Road density	Houston road network dataset
Built environment (5Ds)	Distance to city center	Urban center dataset
Built environment (5Ds)	Transit accessibility	Bus stop dataset
Vegetation	Tree canopy coverage	NLCD Tree Canopy dataset (USA)
Vegetation	Distance to green space	Green land / park dataset

Table 1: Built environment (5Ds) and vegetation variables used in the analysis.

Spatial and Vertical Distribution of WGVI

Figure 5 maps WGVI across floor levels. WGVI generally increases with floor height in low- and mid-rise buildings, indicating improved visual access to vegetation. This pattern is absent in high-rise buildings, where greenery visibility does not consistently increase with floor level.

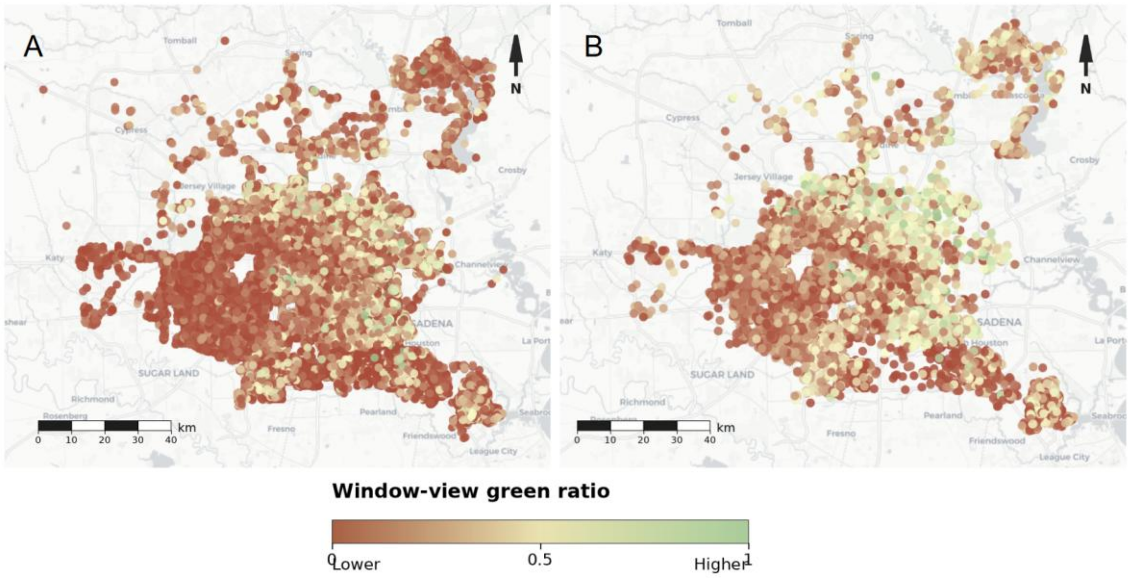

Figure 5: Spatial comparison of WGVI across floor levels: (A) first floor and (B) third floor.

Note: Red indicates lower and green indicates higher WGVI (0-1).

Figure 6 aggregates WGVI by building height and floor level. Mean WGVI rises from 18.6% on the first floor to 26.7% on the second in low-rise buildings, and from 16.6% to about 37% by the seventh floor in mid-rise buildings. High-rise buildings rise from 13.0% to 34.2% by the seventh floor, peak near the eleventh, then fall to 18.0% by the sixteenth and about 13% by the nineteenth.

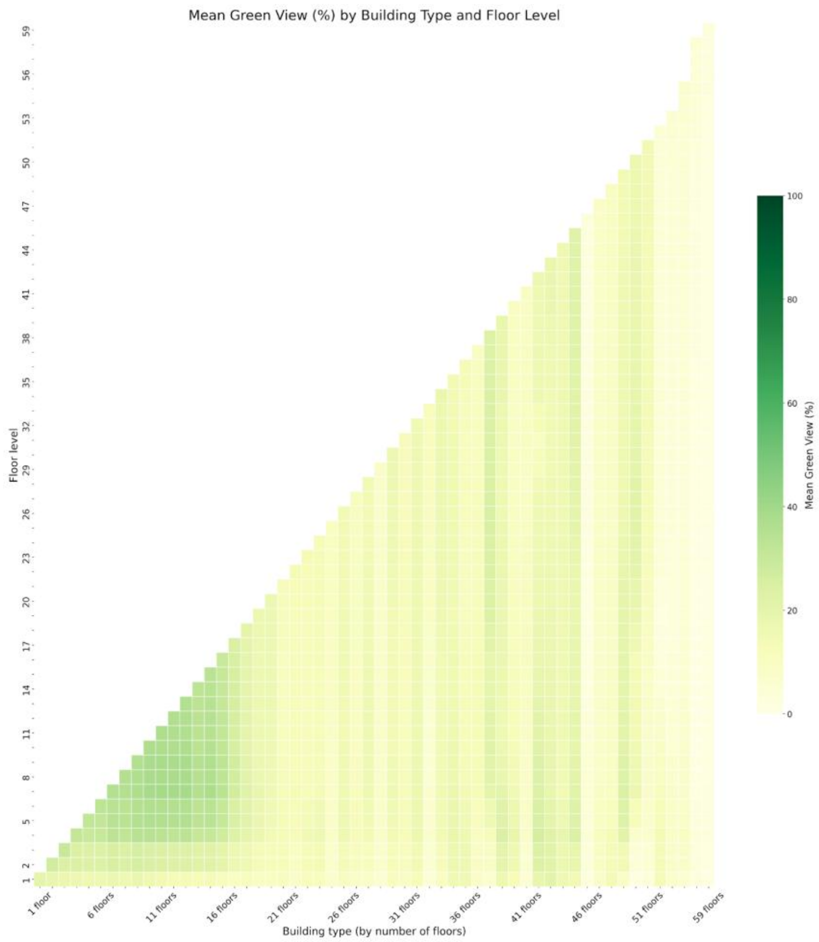

Figure 6: Heatmap of mean WGVI by building height and floor level.

Built Environment and Vegetation Influences on WGVI

To examine the associations between environmental variables and WGVI, Pearson correlation analyses are conducted separately for low-, mid-, and high-rise buildings. Tree canopy coverage is the strongest positive correlate and strengthens with building type (r = 0.22, 0.26, 0.53). Road density is negatively associated and also strengthens (r = -0.11, -0.19, -0.59), as does building height in high-rise buildings (r = -0.54), indicating that surrounding built form governs upper-floor views more than vegetation supply does.

Sensitivity analysis. Because viewpoints follow a standardized rule rather than surveyed windows, we bound the uncertainty using the spread among rendered viewpoints. Within one façade and floor the standard deviation is 4.7 percentage points (pp); across all façades of a building floor it is 10.5 pp. At a median of eight viewpoints per building floor, the standard error of a floor mean is 1.7–3.7 pp. WGVI shifts 2.2 pp per metre vertically, so a 3.5 m rather than 3.0 m floor height would move a fifth-floor estimate by about 5.6 pp. Façade orientation, not lateral window position, dominates within-floor variation.

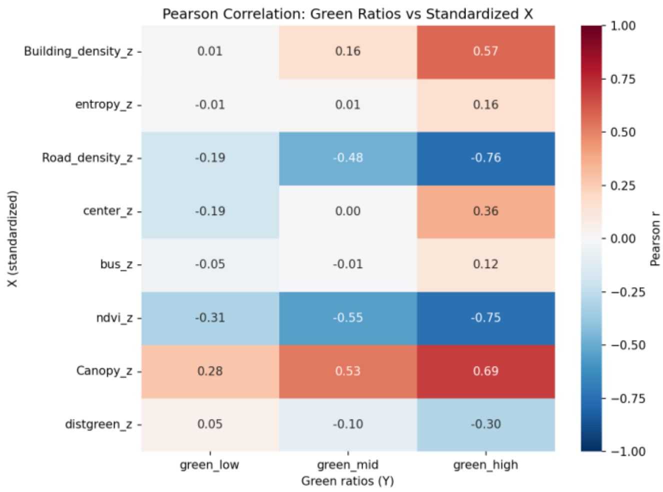

Figure 7: Pearson correlation coefficients between WGVI and standardized environmental variables across building types.

Discussion and Conclusion

This study quantifies window-view green visibility from simulated indoor perspectives in Houston. H1 is partially supported: WGVI increases with floor height in low- and mid-rise buildings but not monotonically in high-rise buildings, where it peaks near the eleventh floor and then declines. H2 is supported: tree canopy coverage is positively associated with WGVI while road density and building height are negatively associated, and all three strengthen with building type, so upper-floor views are governed more by built form than by vegetation supply. Three limitations define the next steps. First, the viewpoint rule samples each building's top floor above its roof; we will re-render at 3.0(k-1) + 1.5 m. Second, WGVI is unvalidated against real imagery; we will match ground-floor viewpoints to street-view panoramas and add on-site photography. Third, the segmentation model is tuned on Hong Kong views, so we will re-tune it on annotated Houston renders.

Acknowledgements:

The authors declare no conflicts of interest. This research is supported by the U.S. National Science Foundation (2318206) and the NASEM Gulf Research Program (SCON-10000653; SCON-10001536).

References

Biljecki, F., & Ito, K. (2021). Street view imagery in urban analytics and GIS: A review. *Landscape and Urban Planning, 215*, 104217. https://doi.org/10.1016/j.landurbplan.2021.104217

Bolte, A.-M., Niedermann, B., Kistemann, T., Haunert, J.-H., Dehbi, Y., & Kotter, T. (2024). The green window view index: automated multi-source visibility analysis for a multi-scale assessment of green window views. *Landscape Ecology, 39*(3). https://doi.org/10.1007/s10980-024-01871-7

Elsadek, M., Liu, B., & Xie, J. (2020). Window view and relaxation: Viewing green space from a high-rise estate improves urban dwellers' wellbeing. *Urban Forestry & Urban Greening, 55*, 126846. https://doi.org/10.1016/j.ufug.2020.126846

He, S., Wang, X., Dong, J., Wei, B., Duan, H., Jiao, J., & Xie, Y. (2019). Three-dimensional urban expansion analysis of valley-type cities: A case study of Chengguan District, Lanzhou, China. *Sustainability, 11*(20), 5663. https://doi.org/10.3390/su11205663

Klepeis, N. E., Nelson, W. C., Ott, W. R., Robinson, J. P., Tsang, A. M., Switzer, P., Behar, J. V., Hern, S. C., & Engelmann, W. H. (2001). The National Human Activity Pattern Survey (NHAPS): a resource for assessing exposure to environmental pollutants. *Journal of Exposure Science & Environmental Epidemiology, 11*(3), 231–252. https://doi.org/10.1038/sj.jea.7500165

Li, M., Xue, F., Wu, Y., & Yeh, A. G. O. (2022). A room with a view: Automatic assessment of window views for high-rise high-density areas using City Information Models and deep transfer learning. *Landscape and Urban Planning, 226*, 104505. https://doi.org/10.1016/j.landurbplan.2022.104505

Li, M., Yeh, A. G. O., & Xue, F. (2024). CIM-WV: A 2D semantic segmentation dataset of rich window view contents in high-rise, high-density Hong Kong based on photorealistic city information models. *Urban Informatics, 3*(1). https://doi.org/10.1007/s44212-024-00039-7

Lin, T.-Y., Le, A.-V., & Chan, Y.-C. (2022). Evaluation of window view preference using quantitative and qualitative factors of window view content. *Building and Environment, 213*, 108886. https://doi.org/10.1016/j.buildenv.2022.108886

Yan, J., Huang, X., Wang, S., He, Y., Li, X., Hohl, A., Li, X., Aly, M., & Lin, B. (2023). Toward a comprehensive understanding of eye-level urban greenness: a systematic review. *International Journal of Digital Earth, 16*(2), 4769–4789. https://doi.org/10.1080/17538947.2023.2283479

Zhu, X. X., Chen, S., Zhang, F., Shi, Y., & Wang, Y. (2025). GlobalBuildingAtlas: An open global and complete dataset of building polygons, heights and LoD1 3D models. *ArXiv*. https://arxiv.org/abs/2506.04106